

# How to use the CD-ROM

## Arrangement of Data

Each semiconductor is labelled by a number "x.y", where x gives the number of the *substance group* ("Elements of the IVth group", "III-V compounds" etc.) and y the number of the *substance* ("C", "Si", "Ge" etc.) within the group.

For each substance the individual data are listed in six *property groups*:

- **Crystal structure** (lattice structure / space group / modifications / high temperature and high pressure phases).
- **Electronic properties** (band structure / energies at symmetry points of the band structure / energy gaps (direct energy gap, indirect energy gap) / exciton energies / intra conduction band energies / intra valence band energies / critical point energies / spin-orbit splitting energies / camel's back structure of the conduction band edge / structure of the top of the valence band / effective masses (electrons, holes) / g-factor of electrons / valence band parameters).
- **Lattice properties** (lattice parameters / linear thermal expansion coefficient / density / melting point / Debye temperature / heat capacity / phonon dispersion relations / phonon frequencies (wavenumbers) / sound velocities / second and third order elastic moduli / bulk modulus / Poisson ratio / internal strain parameter).
- **Transport properties** (electrical conductivity or resistivity (intrinsic conductivity) / (intrinsic) carrier concentration / carrier mobilities (electron mobility, hole mobility) / drift velocities and diffusion constants / thermal conductivity (resistivity) / Seebeck coefficient (thermoelectric power) / piezo- and elastoresistance coefficients).
- **Optical properties** (optical constants / absorption coefficient / reflectance / extinction coefficient / refractive index / dielectric function / dielectric constants / piezo- and elastooptic coefficients).
- **Impurities and defects** (binding energies of impurities / energy levels of impurities, defects and complexes or of deep centers).

If only few data are available some of the property groups are omitted or put together.

## Location of substances

To locate a substance you can open directly the bookmark "Data" and navigate via the bookmarks for the substance groups to the substances and from these to the property groups, references and figures.

Two bookmarks in the start program can help you to locate a substance you are interested in:

### A. Navigation via substance groups

If you open the bookmark "Navigation via substance groups" a list of all semiconductors dealt with in this handbook is shown on the desktop ordered by 38 substance groups:

#### 1 Elements of the IVth group and IV-IV compounds

1.1 C (Diamond)	1.3 Ge	1.5 SiC
1.2 Si	1.4 Sn (grey Sn)	1.6 Si <sub>x</sub> Ge <sub>1-x</sub>

#### 2 III-V compounds

2.1 BN	2.6 AlP	2.11 GaAs	2.16 InSb
2.2 BP	2.7 AlAs	2.12 GaSb	2.17 Al <sub>0.48</sub> In <sub>0.52</sub> As
2.3 BAs	2.8 AlSb	2.13 InN	2.17 Al <sub>0.49</sub> In <sub>0.51</sub> P
2.4 BSb	2.9 GaN	2.14 InP	2.17 AlAs <sub>0.96</sub> P <sub>0.04</sub>
2.5 AlN	2.10 GaP	2.15 InAs	.....

#### 3 II-VI compounds

.....

.....

.....

.....

By clicking on the substance number the first data page of the respective substance is opened. In the bookmark list on the left side of the desktop the respective bookmark is marked, and you can easily open the sub-bookmarks for the property groups, references and figures.

## B. Navigation via element systems

If you open the bookmark "Navigation via element systems" a list of all semiconductors dealt with in this handbook is shown on the desktop ordered alphabetically by the elements the substances are consisting of:

<b>Ag–As–S</b>	AgAsS <sub>2</sub>	28.1
	Ag <sub>3</sub> AsS <sub>3</sub>	28.14
<b>Ag–As–Se</b>	AgAsSe <sub>2</sub>	28.2
<b>Ag–As–Te</b>	AgAsTe <sub>2</sub>	28.3
.....	.....	.....

By clicking on the substance number the first data page of the respective substance is opened. In the bookmark list on the left side of the desktop the respective bookmark is marked, and you can easily open the sub-bookmarks for the property groups, references and figures.

## 1.3 Germanium, Ge

### Crystal structure

The element germanium crystallizes under normal conditions in the diamond lattice (space group: cubic  $O_h^7$  – Fd3m), see Fig. 1.0.2.

### high pressure phases

Under pressure there is a transition from the diamond structure (Ge-I) to the tetragonal  $\beta$ -tin structure (Ge-II) around 10 GPa [63J, 78A, 84O, 86M]. Around 75 GPa there is a transformation from the  $\beta$ -Sn structure (Ge-II) to the simple hexagonal (sh) structure [86V], and around 100 GPa to an intermediate structure, and to the hexagonal close-packed structure [86V]. Recently it has been found that the  $\beta$ -tin transforms continuously to the hexagonal phase via an intermediate phase with Imma structure, as previously found in Si, predicted by [94L] and experimentally found by [96N]; this phase is not a mixture of the  $\beta$ -tin and hexagonal phases [96N]; a high-pressure double-hexagonal close-packed (dhcp) structure has been found above 100 GPa [86V].

Upon depressurising the Ge-II modification, Ge-III (ST12 structure, simple tetragonal with 12 nearest neighbours, space group  $P4_32_12$ ,  $D_4^8$ ) is obtained at RT [63B, 64K, 65B, 83Q, 86M2], a mixture of Ge-III and Ge-IV at 170 ... 200 K, nearly pure Ge-IV (BC8 structure, body centred cubic with 8 nearest neighbours, space group  $Ia\bar{3}$ ,  $T_h^7$ ) at 160 ... 170 K, a mixture of Ge-IV and a glassy phase at 130 ... 160 K, and mostly glassy Ge at 90 ... 130 K [92B].

### Electronic properties

**band structure** : Fig. 1.0.10, Brillouin zone: Fig. 1.0.6

**density of states** in valence and conduction bands: Fig. 1.3.1.

The conduction band is characterized by eight equivalent minima at the end points L of the [111]-axes of the Brillouin zone (symmetry:  $L_6^-$ ). The surfaces of constant energy are ellipsoids of revolution with their major axes along [111]. Higher energy minima of the conduction band are located at  $\Gamma$  and (above these) on the [100]-axes. The valence band is of the general structure shown in Fig. 1.0.7 with its maximum at  $\Gamma$  (symmetry:  $\Gamma_8^+$ ), the light and heavy hole bands being degenerate at this point. Both bands are warped. The third spin-orbit split-off band has  $\Gamma_7^+$  symmetry. In contrast to silicon the spin-orbit splitting energies are considerable. Thus, the symmetry notation of the double group of the diamond lattice is mostly used for Ge.

**energies of symmetry points of the band structure** ( $E$  relative to the top of the valence band)

$E(\Gamma_{6v})$	– 12.66 eV	theoretical data, Fig. 1.0.10a	76C
$E(\Gamma_{7v})$	– 0.29 eV		
$E(\Gamma_{8v})$	0.00 eV		
$E(\Gamma_{7c})$	0.90 eV		
$E(\Gamma_{6c})$	3.01 eV		
$E(\Gamma_{8c})$	3.22 eV		
$E(X_{5v})$	– 8.65 eV		
$E(X_{5v})$	– 3.29 eV	for experimental data from angular	
$E(X_{5c})$	1.16 eV	resolved photoemission, see Fig. 1.0.10b	
$E(L_{6v})$	– 10.39 eV	[85W] and [84H, 85N]	
$E(L_{6v})$	– 7.61 eV		
$E(L_{6v})$	– 1.63 eV		
$E(L_{4,5v})$	– 1.43 eV		
$E(L_{6c})$	0.76 eV		

### indirect energy gap

$E_{g,ind}(\Gamma_{8v}^+ - L_{6c}^-)$	0.744(1) eV 0.664 eV	$T = 1.5$ K $T = 291$ K	magnetotransmission	59Z
$E_{g,th}$	0.785 eV	$T = 0$ K (extrapol.)	temperature dependence of the intrinsic conductivity	54M1

For  $E_{g,ind}(T)$  below 425 K, see Fig. 1.3.2.

## direct energy gap

$E_{g,dir}$	0.898(1) eV	$T = 1.5$ K	magnetoabsorption	59Z
$(\Gamma_{8v}^+ - \Gamma_{7c}^-)$	0.805(1) eV	$T = 293$ K		

temperature dependence of  $E_{g,dir}$ , see Fig. 1.3.2

## exciton ground state

$E(1S_{3/2}^{3/2}(L_4^+ + L_5^+))$	740.46(3) meV		absorption (at 2.1 K) and luminescence	79M
$E(1S_{1/2}^{3/2}(L_6^+))$	741.58 (3) meV		(at 5.1 K), the energy of the assisting LA(L)-phonon is subtracted, the exchange splitting has not been resolved so far	
$E_b$	4.18 meV		$1S_{3/2}^{3/2}(L_4^+ + L_5^+)$	76A
	3.17 meV		$1S_{1/2}^{3/2}(L_6^+)$	
$E(2S_{3/2}^{3/2})$	1.32 meV		theory including valence band degeneracy and conduction band anisotropy	76A
$E(2S_{1/2}^{3/2})$	0.87 meV			
$E(2P)$	2.35(5) meV	$T = 5$ K	$(2P_{3/2}^{3/2}, 2P_{3/2}^{5/2})$	76B2,
	3.13 (5) meV		$2P_{1/2}^{3/2}$	76L
	3.35(5) meV		$(2P_{3/2}^{5/2}, 2P_{-5/2}^{5/2})$	
	3.42(5) meV		$(2P_{3/2}^{5/2}, 2P_{3/2}^{3/2}), (2P_{-5/2}^{5/2}, 2P_{1/2}^{5/2})$	
			far-infrared absorption	

## critical point energies

$E_1$	2.111(3) eV	RT	from ellipsometric data by a two-dimensional critical point analysis (2D CP)	84V
$E_1 + \Delta_1$	2.298(3) eV	RT	2D CP	
$\Delta_1$	0.187(3) eV	RT	2D CP	
$E'_0$	3.123(19) eV	$T = 100$ K	3D CP	
$E'_0 + \Delta'_0$	3.309(19) eV	$T = 100$ K	3D CP	
$E'_{0,av}$	3.110 eV	RT	2D CP; mean value of $E'_0$ and $E'_0 + \Delta'_0$	
$E_2$	4.368 (4) eV	RT	2D CP	
	4.346(3) eV	RT	1D CP	

## spin-orbit splitting energies

$\Delta_0(\Gamma_{7v}^+ - \Gamma_{8v}^+)$	0.297 eV	$T = 10$ K	electroreflectance	75A
$\Delta'_0(\Gamma_{6c}^- - \Gamma_{8c}^-)$	0.200 eV			
$\Delta_1(\Lambda_{4,5v} - \Lambda_{6v})$	0.184 eV			
$\Delta'_1(L_{4,5c}^- - L_{6c}^-)$	0.266 eV			
$\Delta''_1(L_{4,5v}^- - L_{6v}^-)$	0.228 eV			

## conduction band, effective masses

$m_{n\perp}(L_6)$	0.0823 $m_0$	$T = 120$ K	magnetophonon resonance	82H
	0.0807(8) $m_0$	$T = 30 \dots 100$ K	cyclotron resonance at 891 GHz	76F
$m_{n\parallel}(L_6)$	1.59 $m_0$	$T = 120$ K	magnetophonon resonance	82H
	1.57 (3) $m_0$	$T = 30 \dots 100$ K	cyclotron resonance at 891 GHz	76F
$m_n(\Gamma_7)$	0.0380(5) $m_0$	$T = 30$ K	piezomagnetoreflectance	70A

For the dependence of the transverse electron mass in the  $L_6$ -minima on the energy above the bottom of the band, see Fig. 1.3.3a.

**g-factor of electrons**g<sub>c</sub> – 3.0(2) T = 30 K piezomagnetoabsorption 70A**valence band, effective masses**

$m_{p,l}$	0.0438(3) $m_0$	$T = 4 \text{ K}$ , $B \parallel [100]$	cyclotron resonance	56D
	0.0426(2) $m_0$	$T = 4 \text{ K}$ , $B \parallel [111]$		
	0.0430(3) $m_0$	$T = 4 \text{ K}$ , $B \parallel [110]$		
$m_{p,h}$	0.284(1) $m_0$	$T = 4 \text{ K}$ , $B \parallel [100]$		
	0.376(1) $m_0$	$T = 4 \text{ K}$ , $B \parallel [111]$		
	0.352(4) $m_0$	$T = 4 \text{ K}$ , $B \parallel [110]$		
$m_{so}$	0.095 (7) $m_0$	$T = 30 \text{ K}$	piezomagnetoabsorption	70A

For the dependence of the light hole mass on the energy below the top of the band, see Fig. 1.3.3b.

**valence band parameters**

A	– 13.3	extrapolated using a five level $k \cdot p$ scheme	75W2
B	– 8.57		
C	12.78		

**Lattice properties****lattice parameter**

a	5.6579060 Å	$T = 298.15 \text{ K}$	single crystal	75B
---	-------------	------------------------	----------------	-----

For the temperature dependence of  $a$  in the range 20...812°C, see Fig. 1.3.4.**linear thermal expansion coefficient**

For temperature dependence, see Fig. 1.3.5.

$\alpha$	0.00·10 <sup>–6</sup> K <sup>–1</sup>	$T = 0 \text{ K}$	recommended values	75S2
	5.90·10 <sup>–6</sup> K <sup>–1</sup>	$T = 300 \text{ K}$	from different measurements	
	7.20·10 <sup>–6</sup> K <sup>–1</sup>	$T = 600 \text{ K}$		
	8.51·10 <sup>–6</sup> K <sup>–1</sup>	$T = 1000 \text{ K}$		

**density**

d	5.3234 g/cm <sup>3</sup>	$T = 25^\circ\text{C}$	hydrostatic weighing	52S
---	--------------------------	------------------------	----------------------	-----

**melting point**

$T_m$	1210.4 K		73H
$dT_m/dp$	– 2.04·10 <sup>–3</sup> K atm <sup>–1</sup>		67K

**phonon dispersion curve, one phonon density of states** : Fig. 1.3.6.**phonon frequencies**

$\nu_{LTO}(\Gamma_{25})$	9.02(2) THz	$T = 300 \text{ K}$	coherent inelastic neutron scattering	72N
$\nu_{TA}(X_3)$	2.38(2) THz			
$\nu_{LAO}(X_1)$	7.14(2) THz			
$\nu_{TO}(X_4)$	8.17(3) THz			
$\nu_{TA}(L_3)$	1.87(2) THz			
$\nu_{LA}(L_2)$	6.63(4) THz			
$\nu_{TO}(L_3)$	8.55(3) THz			
$\nu_{LO}(L_1)$	7.27(2) THz			

## sound velocities

$v_1$	$4.9138 \cdot 10^5 \text{ cm s}^{-1}$	$T = 298 \text{ K},$	ultrasound measurement (20 MHz),	63M
$v_2$	$3.5424 \cdot 10^5 \text{ cm s}^{-1}$	$\rho = 45 \Omega \text{ cm}$	n-type samples	
$v_3$	$5.3996 \cdot 10^5 \text{ cm s}^{-1}$		designation: mode/direction of propagation/direction of particle displacement	
$v_4$	$3.5425 \cdot 10^5 \text{ cm s}^{-1}$		$v_1$ : long/[001]/[001], $v_2$ : shear/[001]/[1̄10]	
$v_5$	$2.7458 \cdot 10^5 \text{ cm s}^{-1}$		$v_3$ : long./[110]/[110], $v_4$ : shear/[110]/[001]	
			$v_5$ : shear/[110]/[1̄10]	

## elastic moduli

$c_{11}$	$12.40 \cdot 10^{11} \text{ dyn cm}^{-2}$	$T = 298 \text{ K},$	ultrasound measurement	71B2
$c_{12}$	$4.13 \cdot 10^{11} \text{ dyn cm}^{-2}$	$\rho = 37 \Omega \text{ cm}$	temperature dependence: Figs. 1.3.7a...c	
$c_{44}$	$6.83 \cdot 10^{11} \text{ dyn cm}^{-2}$			

## third order elastic moduli

$c_{111}$	$-7.10(6) \cdot 10^{12} \text{ dyn cm}^{-2}$	$T = 298 \text{ K},$	from ultrasound measurements,	64M
$c_{112}$	$-3.89(3) \cdot 10^{12} \text{ dyn cm}^{-2}$	$\rho = 45 \Omega \text{ cm}$	temperature dependence: Fig. 1.3.8	
$c_{123}$	$-0.18(6) \cdot 10^{12} \text{ dyn cm}^{-2}$			
$c_{144}$	$-0.23(16) \cdot 10^{12} \text{ dyn cm}^{-2}$			
$c_{166}$	$-2.92(8) \cdot 10^{12} \text{ dyn cm}^{-2}$			
$c_{456}$	$-0.53(7) \cdot 10^{12} \text{ dyn cm}^{-2}$			

**Young's modulus, torsion modulus** : see Fig. 1.3.9.

## bulk modulus

$B_S$	$7.502 \cdot 10^{11} \text{ dyn cm}^{-2}$	$T = 298 \text{ K},$	from ultrasound measurements	63M
		$\rho = 45 \Omega \text{ cm}$		

## internal-strain parameter

	0.76(4)	X-ray diffraction	64S
--	---------	-------------------	-----

## Debye temperature

$\Theta_D(0)$	374 K	for $\Theta_D(T)$ , see Fig. 1.3.10	59F
---------------	-------	-------------------------------------	-----

**heat capacity** : Fig. 1.3.11.

## Transport properties

Low field transport is maintained by electrons in the  $L_6^+$  minima of the conduction band and holes near the point  $\Gamma_8^+$  in the valence bands. At room temperature, the mobility of samples with impurity concentrations below  $10^{15} \text{ cm}^{-3}$  is limited essentially by lattice scattering; higher donor or acceptor concentrations result in an increasing influence of impurity scattering. At 77 K, even for doping concentrations below  $10^{13} \text{ cm}^{-3}$  the mobilities depend on the impurity concentration. Low temperatures and high concentrations lead to the replacement of free carrier conduction by impurity conduction.

## intrinsic conductivity

$\sigma_i$	$2.1 \cdot 10^{-2} \Omega^{-1} \text{ cm}^{-1}$	$T = 300 \text{ K}$	for temperature dependence, see Fig. 1.3.12	54M1
------------	---	---------------------	--	------

## intrinsic carrier concentration

$n_i$	$2.33 \cdot 10^{13} \text{ cm}^{-3}$	$T = 300 \text{ K}$	for temperature dependence, see Fig. 1.3.13	54M1
-------	--------------------------------------	---------------------	--	------

The best fit to the curve in Fig. 1.3.13 is given by the empirical expression

$$n_i^2 = 3.10 \cdot 10^{32} T^3 \exp(-0.785/kT) \text{ cm}^{-6} \quad (\text{kT in eV}, T \text{ in K})$$

## electron mobility

$\mu_n$	3800 cm <sup>2</sup> /Vs	$T = 300$ K	lattice mobility determined by conductivity measurements of high purity samples.	54M1
---------	--------------------------	-------------	--	------

Temperature dependence in the range 77...300 K given by  $\mu_n = 4.90 \cdot 10^7 T^{-1.66}$  cm<sup>2</sup>/Vs ( $T$  in K); see also Fig. 1.3.14 and 1.3.15.

## hole mobility

$\mu_p$	1800 cm <sup>2</sup> /Vs	$T = 300$ K	lattice mobility in high purity samples.	54M2
---------	--------------------------	-------------	--	------

Temperature dependence in the range 100...300 K given by  $\mu_p = 1.05 \cdot 10^9 T^{-2.33}$  cm<sup>2</sup>/Vs ( $T$  in K); see also Fig. 1.3.15.

## piezoresistance coefficients

n-type material

$\pi_{11}$	-2.7·10 <sup>-12</sup> cm <sup>2</sup> /dyn	$T = 300$ K	uniaxial tensile stress	54S
$\pi_{12}$	-3.9·10 <sup>-12</sup> cm <sup>2</sup> /dyn	$\rho = 5.7$ Ω cm		
(1/2)( $\pi_{11} + \pi_{12} + \pi_{44}$ )	-71.7·10 <sup>-12</sup> cm <sup>2</sup> /dyn			
(1/2)( $\pi_{11} - \pi_{12} - \pi_{44}$ )	62.0·10 <sup>-12</sup> cm <sup>2</sup> /dyn			

p-type material

$\pi_{11}$	-3.7·10 <sup>-12</sup> cm <sup>2</sup> /dyn	$T = 300$ K	resistivity measurements	
$\pi_{12}$	3.2·10 <sup>-12</sup> cm <sup>2</sup> /dyn	$\rho = 1.1$ Ω cm		
(1/2)( $\pi_{11} + \pi_{12} + \pi_{44}$ )	48.1·10 <sup>-12</sup> cm <sup>2</sup> /dyn			

## elastoresistance coefficients

n-type material

$m_{44}$	-93.0	$T = 300$ K,	calculated from measured	54S
$(m_{11} - m_{12})/2$	0.4	$\rho = 1.5$ Ω cm	piezoresistance coefficients with the	
$(m_{11} + 2m_{12})/3$	-6.6		aid of elastic constants tensor $c_{ij}$	

p-type material

$m_{44}$	65.1	$T = 300$ K		
$(m_{11} - m_{12})/2$	-2.8	$\rho = 1.1$ Ω cm		
$(m_{11} + 2m_{12})/3$	2.0			

## Seebeck coefficient (thermoelectric power) (absolute values)

$S_n$	1.07·10 <sup>-3</sup> V/K	$T = 300$ K, $\rho = 17.0$ Ω cm	temperature difference used: 1.5...4 K	65F
$S_p$	1.06·10 <sup>-3</sup> V/K	$T = 280$ K $\rho = 10.5$ Ω cm	temperature dependence: Fig. 1.3.16	

## thermal conductivity

Temperature dependence: Fig. 1.3.17.

## Optical properties

### optical constants

real and imaginary parts of the dielectric constant measured by spectroscopical ellipsometry,  $n$ ,  $k$ ,  $R$ ,  $K$  calculated from these data [83A2]. See also Fig. 1.3.18.

$hv$ [eV]	$\epsilon_1$	$\epsilon_2$	$n$	$k$	$R$	$K$ [ $10^3$ cm $^{-1}$ ]
1.5	21.560	2.772	4.653	0.298	0.419	45.30
2.0	30.361	10.427	5.588	0.933	0.495	189.12
2.5	13.153	20.695	4.340	2.384	0.492	604.15
3.0	12.065	17.514	4.082	2.145	0.463	652.25
3.5	9.052	21.442	4.020	2.677	0.502	946.01
4.0	4.123	26.056	3.90	3.336	0.556	1352.55
4.5	– 14.655	16.782	1.953	4.297	0.713	1960.14
5.0	– 8.277	8.911	1.394	3.197	0.650	1620.15
5.5	– 6.176	7.842	1.380	2.842	0.598	1584.57
6.0	– 6.648	5.672	1.023	2.774	0.653	1686.84

### refractive index , spectral dependence at RT

$n$	4.00541(11)	$\lambda = 8 \mu\text{m}$	mean values for ten samples from various suppliers measured at 20.0°C	82E1
	4.00412(12)	9 $\mu\text{m}$		
	4.00319(11)	10 $\mu\text{m}$		
	4.00248(10)	11 $\mu\text{m}$		
	4.00194(11)	12 $\mu\text{m}$	temperature coefficient between 20°C and 25°C: $4.0 \cdot 10^{-4} \text{ }^\circ\text{C}^{-1}$	
	4.00151(10)	13 $\mu\text{m}$		

The spectral dependence of  $n$ ,  $k$ , and  $K$  below 10 eV is shown in Fig. 1.3.19. For spectral dependence of  $n$  and  $k$ , see also Fig. 1.3.20. Temperature dependence: Fig. 1.3.21.

### dielectric constant

$\epsilon(\infty)$	16.00	$T = 300 \text{ K}$	capacitance measurement	83S
$d \ln \epsilon(\infty)/dT$	$13.8(8) \cdot 10^{-5} \text{ K}^{-1}$	$T = 77 \dots 400 \text{ K}$	optical interference	59C
		$T [\text{K}]$	$v [\text{MHz}]$	
$\epsilon$	16.5	4.2	750	capacitance bridge
	16.0	4.2	9200	microwave measurement
	16.2	300	9200	
	15.8	77	1	capacitance bridge
				53D

For spectra of the real and imaginary parts of the dielectric constant, see Fig. 1.3.22. Temperature dependence of  $\epsilon(\infty)$ : Fig. 1.3.23.

### elastooptic constants

$p_{11}$	– 0.154	$T = 300 \text{ K},$	interferometric technique	78F
$p_{12}$	– 0.126	$\lambda = 10.6 \mu\text{m}$		
$p_{44}$	– 0.073		polarimetric technique	

### third order susceptibilities

The second order susceptibilities are zero as a result of inversion symmetry. The third order susceptibility has two independent components.

$ \chi_{1111} $	$1.0(5) \cdot 10^{-10} \text{ esu}$	CO <sub>2</sub> laser,	optical third order mixing	69W
$ \chi_{1122} $	$0.6(3) \cdot 10^{-10} \text{ esu}$	$\lambda = 10.6 \mu\text{m},$		
$ \chi_{1111} $	$1 \cdot 10^{-10} \text{ esu}$	$T = 300 \text{ K}$	calculated	70V

## Impurities and defects

### shallow donors binding energies

### binding energies of group V substitutional donors

Impurity	$E_b$ [meV]	$T$ [K]	Experimental method, remarks	Ref.
Theory	9.81		donor effective mass calculation	69F
Sb	10.29	10, 4	optical absorption (photothermal ionization)	75S1, 64R
Bi	12.81	10	optical absorption	64R
P	12.89	10	photoconductivity, absorption	74S
As	14.17	10	absorption	64R

### other shallow single donor binding energies

Impurity	$E_b$ [meV]	$T$ [K]	Remarks	Ref.
Li	10.02	4	photoconductivity, absorption	72S, 78H2
O-Li	10.47	6	piezophotoconductivity	78H2
O-H	12.46	4	photoconductivity	78H1, 80J
D <sub>1</sub>	9.38		photoconductivity, observed in oxygen doped crystals	78C
D <sub>2</sub>	10.75		photoconductivity, observed in oxygen doped crystals	78C
Ia	17.25		photoconductivity, "thermal donor"-related	82C, 84C
Ib	17.6		photoconductivity, "thermal donor"-related	82C, 84C
Ic	18.1		photoconductivity, "thermal donor"-related	82C, 84C

### ground state energies of group VI substitutional donors

Impurity	$E$ [meV]	$T$ [K]	Remarks	Ref.
Se <sup>0</sup>	$E_c - 268.2$	20...160	Hall effect, photoconductivity	59T, 85G 88G, 98O
Se <sup>-</sup>	$E_c - 512.4$	140	DLTS	
Te <sup>0</sup>	$E_c - 93$		Hall effect, photoconductivity,	57A, 59N, 59T, 88G
Te <sup>-</sup>	$E_c - 330$		DLTS	
S <sup>0</sup>	$E_c - 280$		Hall effect, DLTS	88G
S <sup>-</sup>	$E_c - 590$			
O	$E_c - 17$		Hall effect, photoconductivity	61F, 62K, 63W, 82C
	$E_c - 40$			
	$E_c - 200$			
	$E_c - 60...80$			78E
	$E_c - 160...180$			
	$E_c - 16...17.3$	7...40	Absorption, D <sup>0</sup> state of oxygen-related thermal double donor.	84C, 82C
	$E_c - 34...37$	7...40	Singly ionized D <sup>+</sup> state of thermal donor	84C

### shallow acceptors binding energies

### binding energy of group III substitutional acceptors

Impurity	$E_b$ [meV]	$T$ [K]	Remarks	Ref.
Theory	11.2		acceptor EMT calculation	76B1
B	10.82	4, 8	photoconductivity, optical absorption	74H
Al	11.15		full series of EMT	65J
Ga	11.32		like excited states	
In	11.99			
Tl	13.45		optical absorption	65J

## binding energy of other shallow singly charged acceptors

Impurity	$E_b$ [meV]	Remarks	Ref.
H, Si(A <sub>2</sub> /A <sub>1</sub> )	11.66, 10.59	hydrogen-silicon associated quenched-in defect. 1.07 meV ground state splitting due to strain dipole acting on central cell. + 21 μeV isotope shift on deuteration.	78H1, 85H1, 87K, 89D
H, C(A <sub>6</sub> )	12.28, 11.30	1.98 meV ground state tunnel splitting	78H1, 87K
CN	11.32	crystals grown in nitrogen atmosphere in	78H2, 85M, 85H1
substitutional (A <sub>3</sub> , A <sub>5</sub> )		graphite coated crucible. 1.1 meV ground state splitting	
CN	10.77		
interstitial (A <sub>4</sub> )			
A <sub>7</sub>	11.01	no correlation with chemical impurity reported	78H1
SA <sub>1</sub>	8.69, 9.48	crystals quenched from 900°C. Detailed	81K, 81B, 82B
SA <sub>2</sub>	8.86, 9.59	identifications uncertain. SA <sub>1,2</sub> hole	
SA <sub>1</sub> (Ni)	9.02, 9.21, 9.37, 9.62	repulsive cores since binding energy less than effective mass value	
SA <sub>1</sub> (Cu)	9.73, 10.5		
SA <sub>2</sub>	13.89		
SA <sub>2</sub>	14.42		
SA <sub>3</sub>	17.89		
Be, H	11.29, 10.79	Be-doped crystal grown in hydrogen atmosphere, 0.50 meV ground state splitting	85M, 87K
Zn, H	12.53, 9.87	Zn-doped crystal grown in hydrogen atmosphere, 2.66 meV ground state splitting	85M, 87K
A <sub>8</sub>	10.34		
A <sub>9</sub>	10.90		
A <sub>10</sub>	11.45, 12.03	0.58 meV ground state splitting	82D

## group II substitutional double acceptors

### neutral double acceptor binding energies

Impurity	$E_b$ [meV]	T [K]	Remarks	Ref.
Be <sup>0</sup>	24.80	2, 8	optical absorption and/or photoconductivity	67S, 71M, 74H, 83C
Zn <sup>0</sup>	32.98	2, 8	optical absorption and/or photoconductivity	60F, 71M
Mg <sup>0</sup>	35.85		optical absorption and/or photoconductivity	85M
Cd <sup>0</sup>	54.96		optical absorption and/or photoconductivity	71M
Hg <sup>0</sup>	91.65	6...20	optical absorption and/or photoconductivity	67C, 71M
Mn <sup>0</sup>	55		optical absorption and/or photoconductivity	85M

### singly ionized double acceptor binding energies

Impurity	$E_b$ [meV]	T [K]	Remarks	Ref.
Be <sup>-</sup>	58.02		optical absorption	83C
Zn <sup>-</sup>	86.51	8...10	optical absorption, excited states observed	83C, 73B
Cd <sup>-</sup>	160	20	Hall effect, photoconductivity	59T
Hg <sup>-</sup>	230	10	optical absorption	67C
Mn <sup>-</sup>	100			85M

## positively charged multiple acceptor binding energies

Impurity	$E_b$ [meV]	T [K]	Remarks	Ref.
Be <sup>+</sup>	5.1	1.2	photoconductivity	85M, 85L,
Zn <sup>+</sup>	2.0	1.2	photoconductivity	83H
Mg <sup>+</sup>	2.9	1.2	photoconductivity	
Mn <sup>+</sup>	3.2	1.2	photoconductivity	
Hg <sup>+</sup>	12.2	1.2	photoconductivity	
Cu <sup>+</sup>	2.0	1.2	photoconductivity	
Ag <sup>+</sup>	35	10	DLTS	89H

## energy levels of group I substitutional triple acceptors and related complexes

### energy levels of group I impurities

Impurity	$E$ [meV]	T [K]	Remarks	Ref.
Cu <sup>0</sup>	$E_v + 43.25$	20...300	Hall effect, photo conductivity	54D, 57W, 85S1
Cu <sup>-</sup>	$E_v + 330$	20...300		57W, 84P1
Cu <sup>2-</sup>	$E_c - 260, E_v + 410$	20...300		57W, 84P1
Cu donor			Cu interstitial	64H
CuH <sub>2</sub>	$E_v + 16.42, 16.81, 16.92, 10$ 16.96, 17.03, 17.08, 17.14, 17.21, 17.29, 17.70, 17.81		photoconductivity (photothermal ionization) produced by Cu diffusion in hydrogen atmosphere grown crystals	77H1, 86K
CuH	$E_v + 175$			77H1
Cu, (D,H)	$E_v + 18.10$			86K
Cu,(H,T)	$E_v + 18.12$			86K
Cu, D <sub>2</sub>	$E_v + 18.20$			86K
Cu, T <sub>2</sub>	$E_v + 18.24$			86K
Cu, Li <sub>2</sub>	$E_v + 20.41$		assignments of Cu, Li <sub>2</sub> and Cu, (Li, H) may be reversed	85H2
Cu, (Li,H)	$E_v + 25.30$			85H2
Cu, As	$E_v + 10.05/9.15$		split ground state, complex with $C_{3v}$ symmetry, found in Cu and As doped, vacuum grown crystals	96S
Au donor	$E_v + 44$			55D, 57W,
Au <sup>0</sup>	$E_v + 135$			59N, 65O,
Au <sup>-</sup>	$E_c - 215$			87S
Au <sup>2-</sup>	$E_c - 56$		Hall effect, photoconductivity and DLTS, the DLTS data given here have not been corrected for the capture cross section activation energy. All levels are assigned to substitutional Au.	
Ag <sup>0</sup>	$E_v + 116$		Hall effect, DLTS	59N, 89H
Ag <sup>-</sup>	$E_c - 261$			
Ag <sup>2-</sup>	$E_c - 113$			

## energy levels of transition metal impurities

Unless otherwise stated, transition metals give rise to acceptor levels. Ground state energy levels for the two ionization states (where relevant) are given.

Impurity	$E$ [meV]	$T$ [K]	Remarks	Ref.
Cr	$E_v + 70, E_v + 120$		resistivity	59N
Mn	$E_v + 160, E_c - 370$	30...400	resistivity, photoconductivity	55W, 59T
Fe	$E_v + 350, E_c - 270$	30...400	resistivity, photoconductivity	54T, 59T
Co	$E_v + 250, E_c - 300$	77...300	resistivity, Hall effect and photoconductivity	55T, 59T
Co-donor	$E_v + 83$			71B3
Ni <sup>0</sup>	$E_v + 207$		only level found with DLTS in hydrogen free, pure germanium	55T, 59T,
Ni - H	$E_v + 159/E_v + 299$		the two levels correlate with the presence of both nickel and hydrogen	92H, 92Z
Pt	$E_v + 40$		resistivity, three acceptor levels.	59N, 54D
Pd	$E_v + 0.03, E_c - 0.18$		interpretation not clear resistivity, Hall effect	80G

## energy levels of defect centers

Defect	$E$ [meV]	Generation	Remarks	Ref.
Di-vacancy (V <sub>2</sub> )-donor			$E_v + 100, 120, 160$ meV levels are interpreted as di-vacancy–donor complexes and are double acceptors	75M, 77M
	$E_v + 100$	1 MeV	P, As doped Ge	
	$E_v + 120$	$\gamma$ -irr. at 280 K	Sb doped Ge	
	$E_v + 160$		Bi doped Ge	
Group V interstitial	$E_c - 200$	1 MeV	n-Ge, interpreted as structural modification of group V interstitial (D <sub>i</sub> ).	64P, 77M
		$\gamma$ -irr. at 280 K	Anneals at 100.. 160°C. This level can also be introduced by fast neutrons and electron irradiation.	
Acceptors labeled by annealing		$\gamma$ -irr. at 42 K	(a) double acceptors, anneal at 65 K, interpreted as vacancy-interstitial (Frenkel) pair "65 K" defects. (b) acceptors, anneal at 160...200 K, arise from interstitial defects observed in dislocation free, high purity Ge grown in H-atmosphere; also produced by $\gamma$ -irr. of dislocated material.	77M
Di-vacancy (V <sub>2</sub> )-H	$E_v + 80$		Attributed to di-vacancyhydrogen complexes (c.f. di-vacancy-donor complexes above).	77H1, 77H2
	$E_v + 200$		$E_v + 71$ meV obtained if degeneracy factor of 4 assumed.	82E2
Di-vacancy (V <sub>2</sub> )-Li	$E_v + 100$	$\gamma$ -irr. at 280 K	Li doped, high purity Ge; resistivity, Hall effect	77H1
$\gamma$ -irr. Ge	$E_v + 270$	$\gamma$ -irr. at 280 K	acceptor, oxygen related defect	72C
$\gamma$ -irr. Ge	$E_v + 340$	$\gamma$ -irr. at 280 K	acceptor, silicon-self interstitial interaction	77M
$\gamma$ -irr. Ge	$E_c - 80$	$\gamma$ -irr. at 280 K	Hall effect, Ge:Li	81V
$\gamma$ -irr. Ge	$E_v + 230, 380$	$\gamma$ -irr. at 280 K	DLTS	82P1
$\gamma$ -irr. Ge	$E_c - 420$			84P2

$\gamma$ -irr. Ge	$E_c - 200$	$\gamma$ -irr. at 280 K	Sb doped Ge	81T
e <sup>-</sup> -irr. Ge	$E_c - 200, 400$	e <sup>-</sup> -irr.	1.5 MeV irradiation, n-type Ge, DLTS studies	81F, 82F
e <sup>-</sup> -irr. Ge	$E_v + 210, 240,$ 310	e <sup>-</sup> -irr.	10 MeV irradiation, p-type Ge, DLTS	83F1
e <sup>-</sup> -irr. Ge	$E_v + 240, 290$	e <sup>-</sup> -irr.	n-type Ge (As doped)	
e <sup>-</sup> -irr. Ge	$E_c - 260, 370,$ 380, 410	e <sup>-</sup> -irr.		82P2
		e <sup>-</sup> -irr.	3.5 MeV irradiation, DLTS studies	83A1
	$E_c - 190, 260,$ 310, 430	e <sup>-</sup> -irr.	n-type Ge, 430meV trap dominant	83A1
	$E_v + 160, 229,$ 350	e <sup>-</sup> -irr.	p-type Ge, 350 meV trap dominant	83A1
2.4 $\mu$ m infrared absorption band	3...5 MeV e <sup>-</sup> irr. 400 keV proton bombardment		vibrational levels of a complex defect. Attributed to di-vacancies in [75S1]. Anneals at 200 K. The electron irradiation gives rise to acceptor levels at $E_v + 80$ meV, $E_v + 160$ meV. <110> axis from polarization experiments. Di-vacancy suggested.	77G
			IR absorption	82G
	2.72 um infra- red absorption band	fast irr.		75N
Oxygen related defect	$E_c - 0.13, 0.25,$ 0.29	1.5 MeV e <sup>-</sup> -irr.	DLTS studies. Correlations with local mode spectra in [65W] for electron irradiated Ge:O suggested.	83F2
	$E_v + 0.27$ eV (donor)	4 MeV e <sup>-</sup> -irr.	Resistivity	84L
	$E_v + 0.14, 0.20$ (acceptor)			
	$E_c - 200, 220,$ 270, 400	thermal n	DLTS studies As, Sb doped Ge $E_c - 220$ suggested to contain interstitial As	84F
Multi– vacancy complexes	$E_v + 16$	fast n irr.	acceptor levels obtained from Hall effect and resistivity measurements	77D, 55C,
	$E_v + 20$			70T
	$E_v + 14$		17...300 K. Observed in Sb-, As-, Ga- doped Ge. Attributed to multivacancy complexes – independent of impurity content	
	$E_v + 60...80$			
	$E_v + 160...180$			
Edge dis- location (?)	$E_v + 90$	plastically deformed Ge	Hall effect, resistivity	74O, 75L,
	$E_v + 75, 190,$ 270, 390	plastically deformed Ge	DLTS	79S
Screw dislocation	$E_v + 35, 590$	twisted Ge	Hall effect, resistivity	83B
Grownin dislocations			DLTS	75W1
	$E_v + 25, 100$			85S2
"ETI"	$E_c - 90$			
	$E_v + 0.17, 0.36$	Laser irr. Ge	DLTS	83P1
	$E_c - 40...100$		DLTS on ultrapure Ge.	85H2

## References to 1.3

- 52S Straumanis, M. E., Aka, A. Z.: J. Appl. Phys. 23 (1952) 330.  
53D Dunlap, W. C., Watters, R. L.: Phys. Rev. 92 (1953) 1396.  
53F Fine, E. M.: J. Appl. Phys. 24 (1953) 338.  
53M McSkimin, H. J.: J. Appl. Phys. 24 (1953) 988.  
54D Dunlap, W. C.: Phys. Rev. 96 (1954) 40.  
54G Geballe, T. H., Hull, G. W.: Phys. Rev. 94 (1954) 1134.  
54M1 Morin, F. J., Maita, J. P.: Phys. Rev. 94 (1954) 1525.  
54M2 Morin, F. J.: Phys. Rev. 93 (1954) 62.  
54S Smith, C. S.: Phys. Rev. 94 (1954) 42.  
54T Tyler, W. W., Woodbury, H. H.: Phys. Rev. 96 (1954) 874.  
55C Cleland, J. W., Crawford, J. H., Pigg, J. G.: Phys. Rev. 99 (1955) 1170.  
55D Dunlap, W. C.: Phys. Rev. 97 (1955) 664.  
55F Fine, M. E.: J. Appl. Phys. 26 (1955) 862.  
55T Tyler, W. W., Newman, R., Woodbury, H. H.: Phys. Rev. 97 (1955) 669.  
55W Woodbury, H. H., Tyler, W. W.: Phys. Rev. 100 (1955) 659.  
56A D'Altry, F. A., Fan, H. Y.: Phys. Rev. 103 (1956) 1671.  
56D Dexter, R. N., Zeiger, H. J., Lax, B.: Phys. Rev. 104 (1956) 637.  
57A Armstrong, J. A., Tyler, W. W., Woodbury, H. H.: Bull. Am. Phys. Soc. 2 (1957) 265.  
57W Woodbury, H. H., Tyler, W. W.: Phys. Rev. 105 (1957) 84.  
59C Cardona, M., Paul, W., Brooks, H.: J. Phys. Chem. Solids 8 (1959) 204.  
59F Flubacher, P., Leadbetter, A. J., Morrison, J. A.: Philos. Mag. 4 (1959) 273.  
59M McSkimin, H. J.: J. Acoust. Soc. Am. 31 (1959) 287.  
59N Newman, R., Tyler, W. W.: Solid State Physics, Vol. 8, Seitz, F., Turnbull, D. (eds.) New York: Academic Press 1959, p. 49.  
59P Philipp, H. P., Taft, E. A.: Phys. Rev. 113 (1959) 1002.  
59T Tyler, W. W.: J. Phys. Chem. Solids 8 (1959) 59.  
59Z Zwerdling, S., Lax, B., Roth, L. M., Button, K. J.: Phys. Rev. 114 (1959) 80.  
60F Fisher, P., Fan, H. Y.: Phys. Rev. Lett. 5 (1960) 195.  
60L Lukeš, F.: Czech. J. Phys. B 10 (1960) 742.  
60M McLean, T. P.: in Progress in Semiconductors, Vol. 5, A. F. Gibson ed., Heywood, London 1960.  
61F Fuller, C. S., Doleiden, F. H.: J. Phys. Chem. Solids 19 (1961) 251.  
62K Kaiser, W.: J. Phys. Chem. Solids 23 (1962) 255.  
63B Bundy, F. P., Kasper, J. S.: Science 139 (1963) 340.  
63J Jamieson, J. C.: Science 139 (1963) 762.  
63M McSkimin, H. J., Andreatch, Jr., P.: J. Appl. Phys. 34 (1963) 651.  
63P Philipp, H. P., Ehrenreich, H.: Phys. Rev. 129 (1963) 1550.  
63W Whan, R. A., Stein, H. J.: Appl. Phys. Lett. 3 (1963) 187.  
64H Hall, R. N., Racette, J. H.: J. Appl. Phys. 35 (1964) 379.  
64K Kasper, J. S., Richards, S. M.: Acta Crystallogr. 17 (1964) 752.  
64M McSkimin, H. J., Andreatch, Jr., P.: J. Appl. Phys. 35 (1964) 3312.  
64P Pigg, J. C., Crawford, J. H.: Phys. Rev. 135 (1964) A1 141.  
64R Reuszer, J. H., Fisher, P.: Phys. Rev. 135 (1964) A1 125.  
64S Segmüller, A.: Phys. Kond. Mater. 3 (1964) 18.  
65B Bates, C. H., Dachille, F., Roy, R.: Science 147 (1965) 860.  
65F Freud, P. J., Rothberg, G. M.: Phys. Rev. 140 (1965) A1007.  
65J Jones, R. L., Fisher, P.: J. Phys. Chem. Solids 26 (1965) 1125.  
65O Ostroborodova, V. V.: Fiz. Tverd. Tela 7 (1965) 610; Sov. Phys.-Solid State (English Transl.) 7 (1965) 484.  
65W Whan, R. E.: Phys. Rev. 140 (1965) A690.  
66P Potter, R. F.: Phys. Rev. 150 (1966) 562.  
66R Rao, K. V., Smakula, A.: J. Appl. Phys. 37 (1966) 2840.  
67C Chapman, R. A., Hutchinson, W. G.: Phys. Rev. 157 (1967) 615.  
67K Krestronikov, A. N., Ev'genev, S. B., Ulazov, V. M.: Dokl. Akad. Nauk SSSR 174 (1967) 634.  
67S Shenker, H., Swiggard, E. M., Moore, W. J.: Trans. Metall. Soc. AIME 239 (1967) 347.  
68S Singh, H. P.: Acta Crystallogr. 24a (1968) 469.  
69A Aggarwal, R. L., Zuteck, M. D., Lax, B.: Phys. Rev. 180 (1969) 800.  
69F Faulkner, R. A.: Phys. Rev. 184 (1969) 713.  
69W Wynne, J. J.: Phys. Rev. B 1978 (1969) 1295.  
70A Aggarwal, R. L.: Phys. Rev. B 2 (1970) 446.

- 70T Tkachev, V. D., Urenev, V. I.: Fiz. Tekh. Poluprovodn. 4 (1970) 2405; Sov. Phys. Semicond. (English Transl.) 4 (1970) 2075.  
 70V Van Vechten, J. A., Cardona, M., Aspnes, D. E., Martin, R. M. Proc. Int. Conf. Phys. Semicond. 1970, U. S. At. Energy Com., 1970, p. 82.  
 71B1 Buchenauer, C. J., Cerdeira, F., Cardona, M.: in Proc. 2<sup>nd</sup> Int. Conf. Light Scattering in Solids. Balkanski, M. ed., Flammarion, Paris 1971, p. 280.  
 71B2 Burenkov, Yu. A., Nikanorov, S. P., Stepanov, A. V.: Sov. Phys. Solid State (English Transl.) 12 (1971) 1940; Fiz. Tverd. Tela 12 (1970) 2428.  
 71B3 Barnik, M. I., Beglov, D. I., Romanychev, D. A., Kharionovskii, Y. S.: Fiz. Tekh. Poluprovodn. 5 (1971) 106; Sov. Phys. Semicond. (English Transl.) 5 (1971) 87.  
 71M Moore, W. J.: J. Phys. Chem. Solids 32 (1971) 93.  
 71N Nilsson, G., Nelin, G.: Phys. Rev. B 3 (1971) 364.  
 72C Cleland, J. W.: IEEE Trans. Nucl. Sci. N519 (1972) 224.  
 72N Nilsson, G., Nelin, G.: Phys. Rev. B 6 (1972) 3777.  
 72S Seccombe, S. D., Korn, D.: Solid State Commun. 11 (1972) 1539.  
 73H Hultgren, R., Desai, P. D., Hawkins, D. T., Gleiser, M., Kelly, K. K., Wagram, D.: Selected values of the thermodynamic properties of the elements. American Society for Metals, Metals Park, Ohio 1973.  
 74H Haller, E. E., Hansen, W. L.: Solid State Commun. 15 (1974) 687.  
 74L Ley, L., Pollak, R. S., McFeely, F. R., Kowalezyk, S. P., Shirley, D. A.: Phys. Rev. B9 (1974) 600.  
 74O Osipyan, Y. A., Shevchenko, S. A.: Zh. Exp. Teor. Fiz. 65 (1973) 698; Sov. Phys. JETP (English Transl.) 38 (1974) 345.  
 74S Skolnick, M. S., Eaves, L., Stradling, R. A., Portal, J. C., Askenazy, S.: Solid State Commun. 125 (1974) 1403.  
 75A Aspnes, D. E.: Phys. Rev. B12 (1975) 2297.  
 75B Baker, J. F. C., Hart, M.: Acta Crystallogr. 31a (1975) 364.  
 75L Labusch, R., Schroter, W.: Int. Conf. on Defects in Semicond., Freiburg 1974, London and Bristol: Institute of Physics 1975, p. 103.  
 75M Mashovets, T. M., Emstev, V. V.: Int. Conf. on Defects on Semicond., Freiburg 1974, London and Bristol: Institute of Physics 1975, p. 103.  
 75N Newman, R. C., Totterdell, D. H. J.: Int. Conf on Lattice Defects in Semiconductors, Freiburg 1974, Huntley, F. A. (ed.), London and Bristol: Institute of Physics 1975, p. 172.  
 75S1 Skolnick, M. S., Eaves, L., unpublished.  
 75S2 Slack, G. A., Bartram, S. F.: J. Appl. Phys. 46 (1975) 89.  
 75W1 Wagner, R., Hansen, P.: Int. Conf. on Defects in Semicond., Freiburg 1974, London and Bristol: Institute of Physics 1975, p. 387.  
 75W2 Wiley, J. D.: in "Semiconductors and Semimetals", Vol. 10, R. K. Willardson, A. C. Beer eds., Academic Press, New York 1975.  
 76A Altarelli, M., Lipari, N. O.: Phys. Rev Lett. 36 (1976) 619.  
 76B1 Baldereschi, A., Lipari, N. O.: Proc. 13<sup>th</sup> Int. Conf. on the Physics of Semicond. . Rome 1976, Fumi, F. G. (ed.), Marves 1976, p. 595.  
 76B2 Buchanan, M., Timusk, T.: Proc. 13<sup>th</sup> Int. Conf. Physics Semiconductors, Rome 1976, ed. by F. G. Fumi, Marves, p. 821.  
 76C Chelikowski, J. R., Cohen, M. L.: Phys. Rev. B 14 (1976) 556.  
 76F Fink, D., Braunstein, R.: Phys. Status Solidi (b) 73 (1976) 361.  
 76I Icenogle, H. W., Platt, B. C., Wolfe, W. L.: Appl. Opt. 15 (1976) 2348.  
 76L Lipari, N. O., Altarelli, M., Tosatti, E.: Solid State Commun. 21 (1976) 979.  
 77D Dobrego, V. P., Ermdaev, O. P., Tkachev, V. F.: Phys. Status Solidi (a) 44 (1977) 435.  
 77G Gerasimov, A. B., Dolidze, N. D., Konovalenko, B. M.: Fiz. Tekh. Poluprovodn. 11 (1977) 1349; Sov. Phys. Semicond. (English T~ttsl.) 11 (1977) 793.  
 77H1 Haller, E. E., Hubbard, G. S., Hansen, W. L.: IEEE Trans. Nucl. Sci. N524 (1977) 48.  
 77H2 Haller, E. E., Hubbard, G. S., Hansen, W. L., Seeger, A.: Int. Conf. on Radiation Effects in Semiconductors, Dubrovnik 1976, Institute of Physics Conf. Ser. No. 31 1977, p. 309.  
 77M Mashovets, T. M.: Int. Conf. on Radiation Effects in Semiconductors, Dubrovnik 1976. Institute of Physics Couf. Ser. No. 31 1977, p. 30.  
 78A Asaumi, K. A., Minomura, S.: J. Phys. Soc. Jpn. 45 (1978) 1061.  
 78C Clauws, P., van der Steen, K., Broeckx, J., Schoenmaekers, W.: Int. Conf. on Defects and Radiation Effects in Semiconductors, Nice 1978, Institute of Physics Conf. Ser. No. 46, p. 218.

- 78E Emtsev, V. V., Goncharev, L. A., Dostkhodzhoev, T. N.: Fiz. Tekh. Poluprovodn. 12 (1978) 139; Sov. Phys. Semicond. (English Transl.) 12 (1978) 78.
- 78F Feldmann, A., Waxler, R. M., Horowitz, D.: J. Appl. Phys. 49 (1978) 2589.
- 78H1 Haller, E. E.: Phys. Rev. Lett. 40 (1978) 584.
- 78H2 Haller, E. E., Falicov, L. M.: Phys. Rev. Lett. 41 (1978) 1192.
- 79M Martin, T. P., Schaber, H.: Z. Physik B 35 (1979) 61.
- 79S Schroter, W.: Int. Conf. on Defects and Radiation Effects in Semiconductors, Nice 1978, Institute of Physics Conf. Ser. No. 46 1979, p. 114.
- 80G Golubev, N. F., Latyshev, A. V.: Sov. Phys. Semicond. (English Transl.) 14 (1980) 1074.
- 80J Joos, B., Haller, E. E., Falicov, L. M.: Phys. Rev. B22 (1980) 832.
- 80Z Zverev, V. N.: Sov. Phys. Solid State (English Transl.) 22 (1980) 1921; Fiz. Tverd. Tela 22 (1980) 3282.
- 81B Broeckx, J., Kamiura, Y., Clauws, P., Vennik, J.: Solid State Commun. 40 (1981) 149.
- 81F Fukuoka, N., Saito, H.: Jpn. J. Appl. Phys. 20 (1981) L519.
- 81J Jacoboni, C., Nava, F., Canali, C., Ottaviani, G.: Phys. Rev. B 24 (1981) 1014.
- 81K Kamiura, Y., Broeckx, J., Clauws, P., Vennik, J.: Solid State Commun. 38 (1981) 883.
- 81T Tarasik, M. I., Tkachev, V. D., Yavid, V. U., Yanchenko, A. M.: Phys. Status Solidi (0) 104 (1981) K117.
- 81V Vasileva, E. D., Daluda, Y. N., Emstev, V. V., Kervalishvili, P. D., Mashovets, T. V.: Sov. Phys. Semicond. (English Transl.) 15 (1981) 55.
- 82B Broeckx, J., Kamiura, Y., Clauws, P., Vennik, J.: Solid State Commun. 43 (1982) 499.
- 82C Clauws, P., Broeckx, J., Simeon, E., Vennik, J.: Solid State Commun. 44 (1982) 1011.
- 82D Darken, L. S.: J. Appl. Phys. 53 (1982) 3754.
- 82E1 Edwin, R. P., Dudermel, M. T., Lamare, M.: Appl. Optics 21 (1982) 878.
- 82E2 Emstev, V. V., Mashovets, T. V., Nazaryan, E. K., Haller, E. E.: Sov. Phys. Semicond. (English Transl.) 16 (1982) 182.
- 82F Fukuoka, N., Saito, H.: Jpn. J. Appl. Phys. 21 (1982) 930.
- 82G Gerasimov, A. B., Dolidze, N. D., Donina, R. M., Konovalenko, B. M., Ofengein, G. L., Tsartsadze, A. A.: Phys. Status Solidi (a) 70 (1982) 23.
- 82H Hirose, Y., Shimomac, K., Hamaguchi, C.: J. Phys. Soc. Jpn. 51 (1982) 2226.
- 82P1 Pearton, S. J., Tavendale, A. J., Williams, A. A.: Radiat. Eff. 60 (1982) 129.
- 82P2 Poulin, F., Bourgoin, J. C.: Phys. Rev. B26 (1982) 6788.
- 83A1 Aeshin, A. I., Smirnov, L. S., Stas, V. F.: Sov. Phys. Semicond. (English Transl.) 17 (1983) 977.
- 83A2 Aspnes, D. E., Studna, A. A.: Phys. Rev. B 27 (1983) 985.
- 83B Baumann, F. H., Schroter, W.: Phys. Status Solidi (a) 79 (1983) K123.
- 83C Cross, J. W., Holt, L. T., Ramdas, A. K., Sauer, R., Haller, E. E.: Phys. Rev. B28 (1983) 6953.
- 83F1 Fukuoka, N., Saito, H.: Physica 116B (1983) 343.
- 83F2 Fukuoka, N., Saito, H.: Jpn. J. Appl. Phys. 22 (1983) L353.
- 83H Haller, E. E., McMurray, R. E., Falicov, L. M., Haegel, N. M., Hansen, W. L.: Phys. Rev. Lett. 51 (1983) 1089.
- 83P1 Pearton, S. J., Tavendale, A. J.: J. Appl. Phys. 54 (1983) 440.
- 83P2 Philip, J., Breazeale, M. A.: J. Appl. Phys. 54 (1983) 752.
- 83Q Qadri, S. B., Skelton, E. F., Webb, A. W.: J. Appl. Phys. 54 (1983) 3609; see also Spain, I. L., Qadri, S. B., Menoni, C. S., Webb, A. W., Skelton, E. F.: in "Physics of Solids under High Pressure", Schilling, J. S., Shelton, R. N. (eds.), North-Holland, Amsterdam, 1982, p. 73.
- 83S Samara, G. A.: Phys. Rev. B 27 (1983) 3494.
- 84B Bakhchieva, S. R., Kekelidze, N. P., Kekua, M. G.: Phys. Status Solidi (a) 83 (1984) 139
- 84C Clauws, P., Vennik, J.: Phys. Rev. B30 (1984) 4837.
- 84F Fukuoka, N., Saito, H.: Jpn. J. Appl. Phys. 23 (1984) 203.
- 84H Hsieh, T. C., Miller, T., Chiang, T. C.: Phys. Rev. B 30 (1984) 7005.
- 84L Litvinov, V. V., Urenev, V. I., Shershel, V. A.: Sov. Phys. Semicond. (English Transl.) 18 (1984) 707.
- 84O Olijnuk, H., Sikka, S. K., Holzapfel, W. B.: Phys. Lett. 103A (1984) 137; Olijnyk, H., Holzapfel, W. B.: J. Phys. (Paris) 45 Suppl., Colloq. C8 (1984) C8-153.
- 84P1 Pearton, S. J., Haller, E. E., Kahn, J. M.: J. Phys. C17 (1984) 2375.
- 84P2 Pearton, S. J., Tavendale, A. J., Kahn, J. M., Haller, E. E.: Radiat. Eff. 81 (1984) 293.
- 84V Vina, L., Logothetidis, S., Cardona, M.: Phys. Rev. B 30 (1984) 1979.
- 85G Grimmeiss, H. G., Larsson, K., Montelius, L.: Solid State Commun. 54 (1985) 863.
- 85H1 Haller, E. E. in: Microscopic identification of electronic defects in semiconductors, MRS Symposia Proceedings, Vol. 46, Johnson, N. M., Bishop, S. G., Watkins, G. D. (eds.), 1985, p. 495.
- 85H2 Hubbard, G. S., Haller, E. E., Pearton, S. J.: IEEE Trans. Nucl. Sci. N532 (1985) 549.
- 85K Kagaya, H.-M., Soma, T.: Phys. Status Solidi (b) 127 (1985) K5.

- 85L Labrie, D., Thewalt, M. L. W., Clayman, B. P., Timusk, T.: Phys. Rev. B32 (1985) 5514  
85M McMurray, R. E.: Solid State Commun. 53 (1985) 1127.
- 85N Nichols, J. M., Hansson, G. V., Karlsson, U. O., Persson, P. E. S., Uhrberg, R. I. G., Engelhard, R., Flodström, S. A., Koch, E. E.: Phys. Rev. B 32 (1985) 6663.
- 85S1 Salib, E. H., Fisher, P., Simmonds, P. E.: Phys. Rev. B32 (1985) 2424.
- 85S2 Simeon, E., Clauws, P., Vennik, J.: Solid State Commun. 54 (1985) 1025.
- 85W Wachs, A. L., Miller, T., Hsieh, T. C., Shapiro, A. P., Chiang, T. C.: Phys. Rev. B 32 (1985) 2326.
- 86K Kahn, J. M., Falicov, L. M., Haller, E. E.: Phys. Rev. Lett. 57 (1986) 2077.
- 86M Menoni, C. S., Hu, J. Z., Spain, I. L.: Phys. Rev. B 34 (1986) 362.
- 86V Vohra, Y. K., Brister, K. E., Desgreniers, S., Ruoff, A. L., Chang, K. J., Cohen, M. L.: Phys. Rev. Lett. 56 (1986) 1944.
- 87K Kahn, J.M., McMurray, Jr., R.E., Haller, E.E., Falicov, L.M., Phys. Rev. B 36 (1987) 8001.
- 87S Simoen, E., Clauws, P., Huylebroeck, G., Vennik, J., Semicond. Sci. Technol. 2 (1987) 507.
- 88G Grimmeis, H., Montelius, L., Larsson, K.: Phys. Rev. B37 (1988) 6916.
- 89D Denteneer, P. J. H., Van de Walle, C. G., Pantelides, S. T., Phys. Rev. Lett. 62 (1989) 1884.
- 89H Huylebroeck, G., Clauws, P., Simoen, E., Rotsaert, E., Vennik, J., Semicond. Sci. Technol. 4 (1989) 529.
- 91G Giannozzi, P., de Gironcoli, S., Pavone, P., Baroni, S.: Phys. Rev. B 41 (1991) 7231.
- 92B Brazhkin, V. V., Lyapin, A. G., Popova, S. V., Voloshin, R. N.: Pisma Zh. Ekspres. Teor. Fiz. 56 (1992) 156; JETP Letters 56 (1992) 152 (Engl. Transl.); Brazhkin, V. V., Lyapin, A. G., Popova, S. V.: in: "High Pressure in Materials Science and Geoscience" (XXXII. Annual Meeting EHPRG), Kamarad, J. et al. (eds.) (1994) 65.
- 92H Huylebroeck, G., Clauws, P., Simoen, E., Vennik, J. Solid State Commun. 82 (1992) 367.
- 92Z Zach, F.X., Grimmeiss, H., Haller, E.E., Materials Science Forum 83-87 (1992) 245.
- 94L Lewis, S. P., Cohen, M. L.: Solid State Commun. 89 (1994) 483.
- 96K Klotz, S., Besson, J. M., Braden, M., Karch, K., Bechstedt, F., Strauch, D., Pavone, P.: Phys. Status Solidi (b) 198 (1996) 105.
- 96N Nelmes, R. J., Liu, H., Belmonte, S. A., Loveday, J. S., McMahon, M. I., Allan, D. R., Häusermann, D., Hanfland, M.: Phys. Rev. B 53 (1996) R2907.
- 96S Sirmain, G., Dubon, O.D., Hansen, W.L., Olsen, C.S., Haller, E.E., J. Appl. Phys. 79 (1996) 209.
- 98O Olsen, C.S., Beeman, J.W., Itoh, K.M., Farmer, J., Ozhogin, V.I., Haller, E.E.: Solid State Commun. 108 (1998) 895.

## Figures to 1.3

**Fig. 1.0.2**

The diamond lattice. The elementary cubes of the two face-centered cubic lattices are shown.

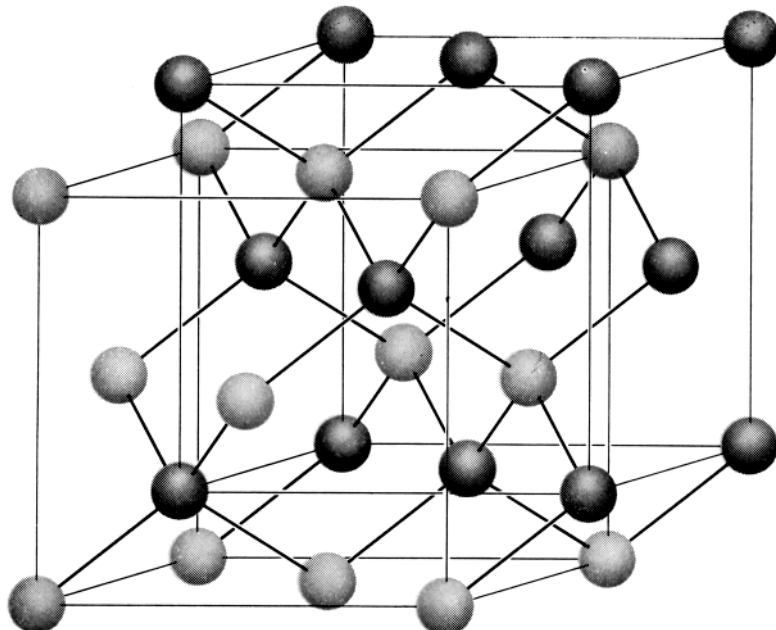


**Fig. 1.0.6**

Brillouin zone of the diamond lattice

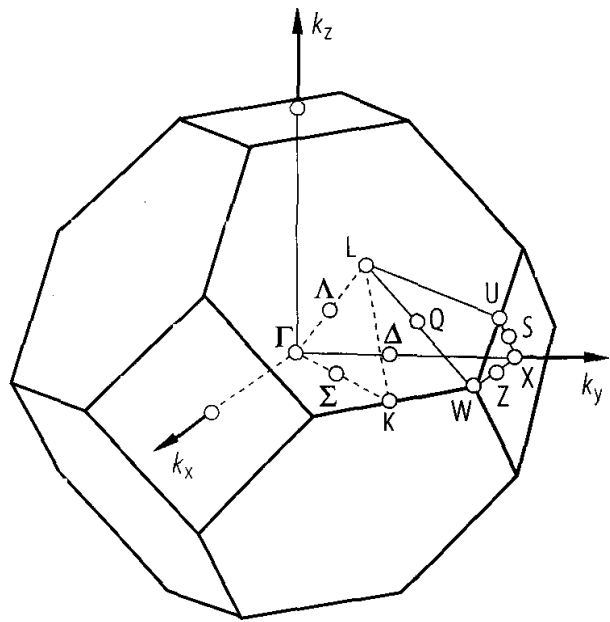


**Fig. 1.0.10**

Ge. (a) Band structure obtained by a non-local pseudopotential calculation including spin-orbit interaction [76C], (b) comparison of the calculated valence bands along the  $\Delta$ - and  $\Lambda$ -axes with angular resolved photoemission data [85W].

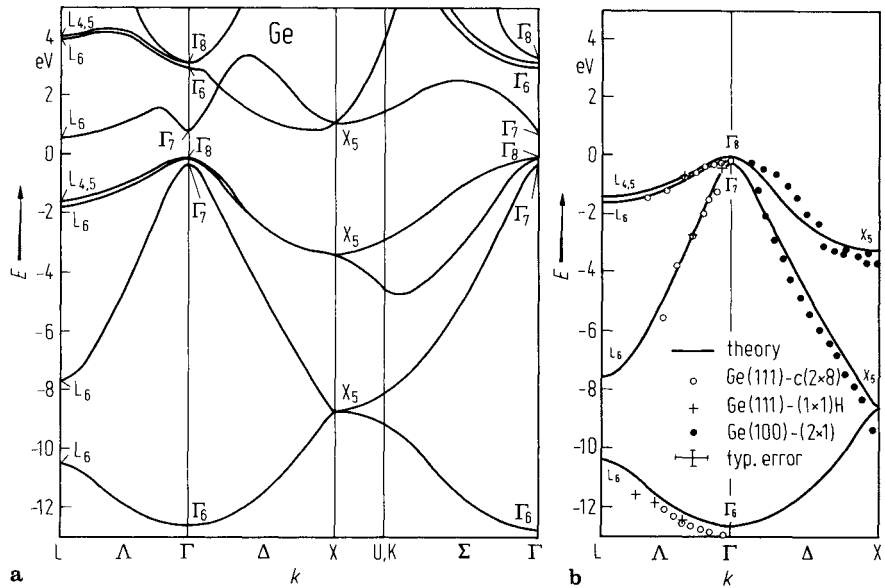


**Fig. 1.3.1**

Ge. Density of states of valence and conduction bands (solid line: obtained by a non-local pseudopotential calculation [76C], dashed line: XPS spectra showing the valence band density of states [74L]).  $E - E_v$  in eV.

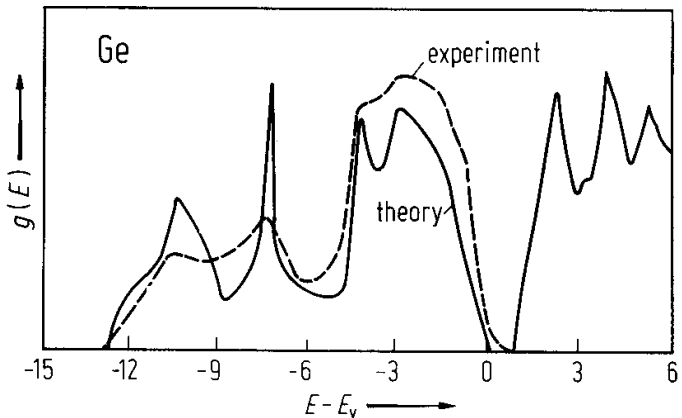


**Fig. 1.3.2**

Ge. Indirect and direct energy gaps vs. temperature [60M].

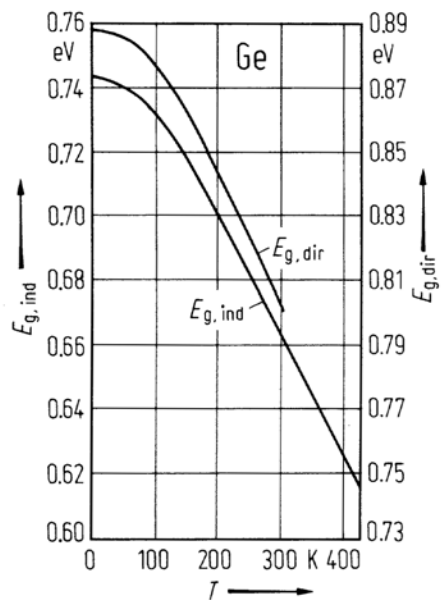


**Fig. 1.3.3**

Ge. (a) Dependence of the transverse electron mass in the  $L_6$  minima on energy above the bottom of the conduction band measured by magnetopiezotransmission [69A], (b) cyclotron mass of light holes vs. energy below the top of the valence band ( $B \parallel [111]$ , [110] and [100]) [80Z].

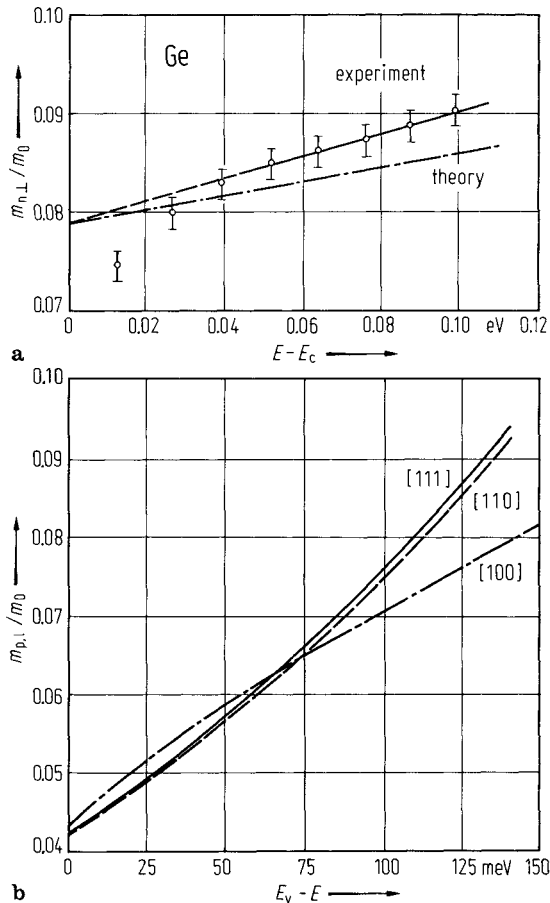


**Fig. 1.3.4**

Ge. Lattice parameter vs. temperature [68S].

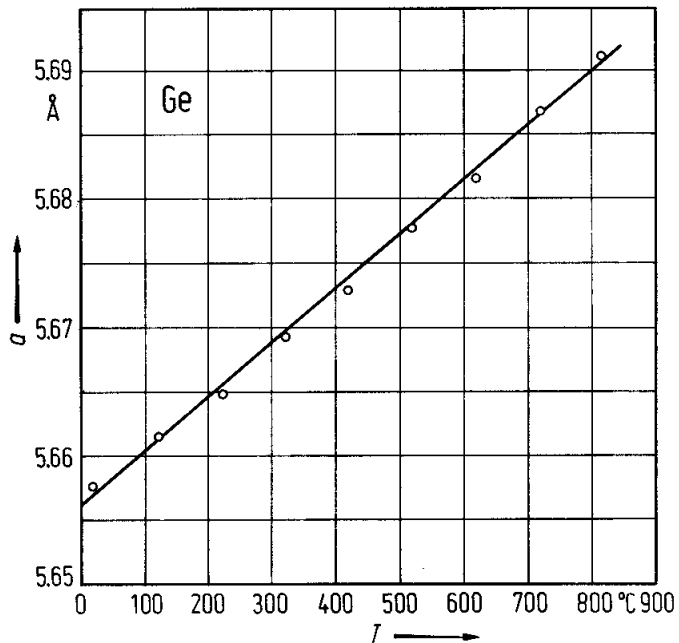


**Fig. 1.3.5**

Ge. Linear thermal expansion coefficient vs. temperature. Experimental data from various authors and theoretical results (solid line) [85K].

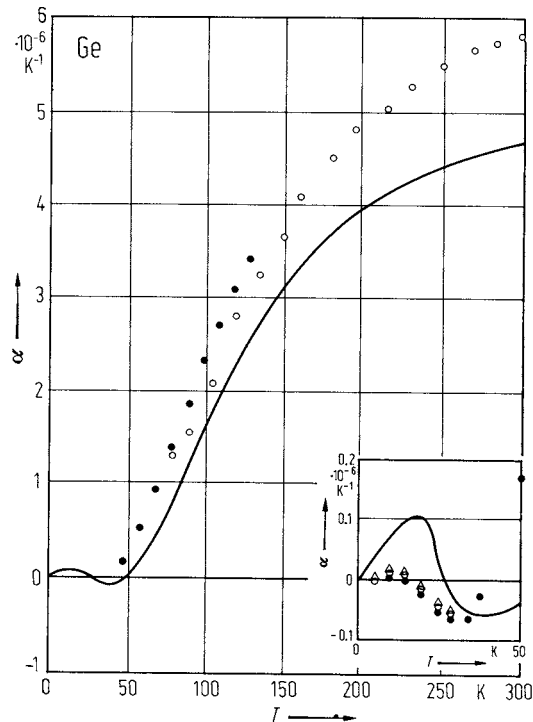


**Fig. 1.3.6**

Ge. Phonon dispersion curves (left panel) and phonon density of states (right panel) [91G]. Experimental data points [71N] and ab-initio calculations [91G].

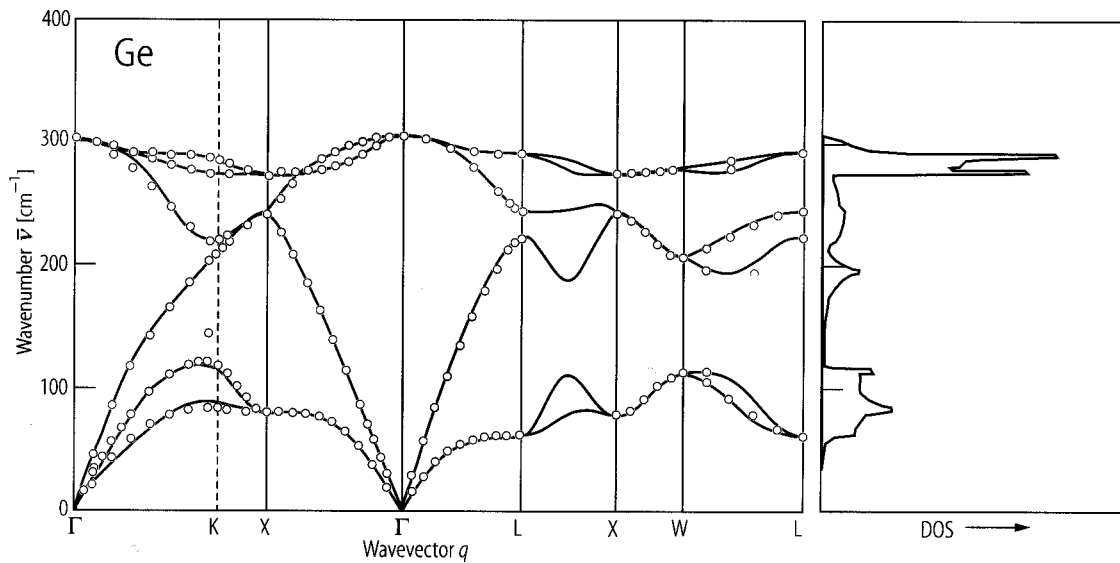


**Fig. 1.3.7a** Ge. Elastic modulus  $c_{11}$  vs. temperature [53M].

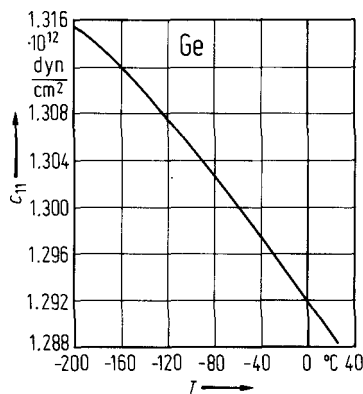


**Fig. 1.3.7b** Ge. Elastic modulus  $c_{12}$  vs. temperature [53M].

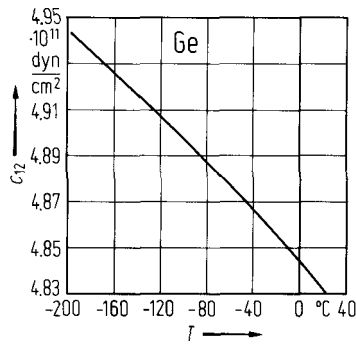


**Fig. 1.3.7c** Ge. Elastic modulus  $c_{44}$  vs. temperature [53M].

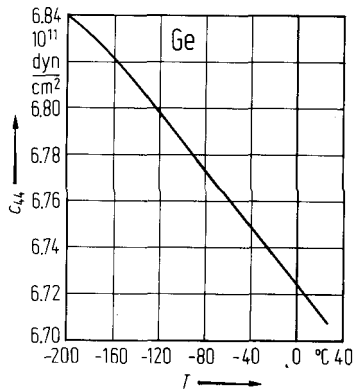


**Fig. 1.3.8**

Ge. Third-order elastic moduli vs. temperature. Solid lines: best fit to the data [83P2].

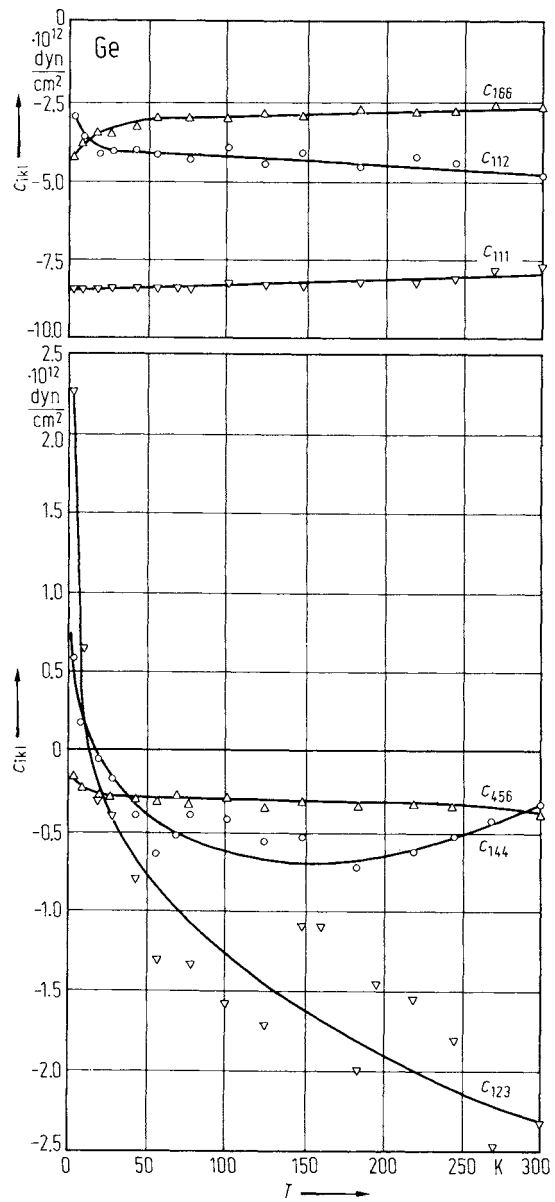


**Fig. 1.3.9**

Ge. Young's moduli  $E$  and torsion modulus  $G$  vs. temperature according to [71B1] (1); [53F, 55F] (2); [53M, 59M] (3).

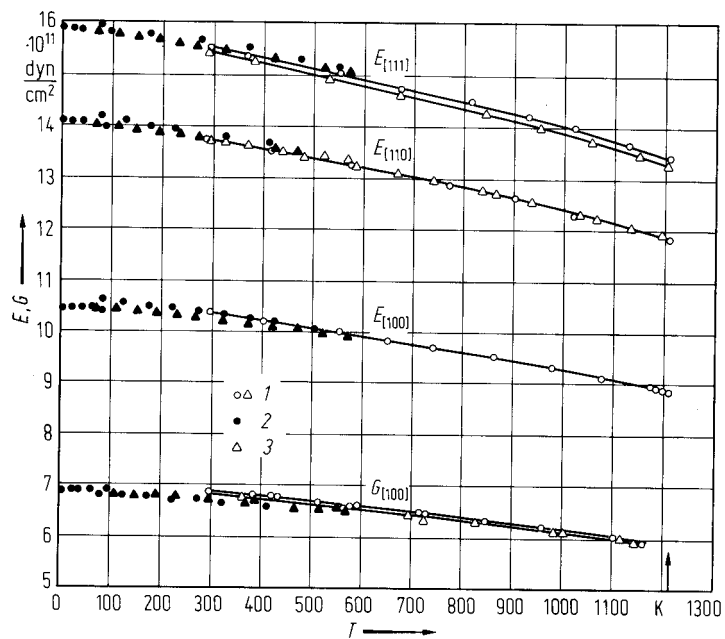


**Fig. 1.3.10**

Ge. Debye temperature  $\Theta_D(T)$  vs. temperature [59F].

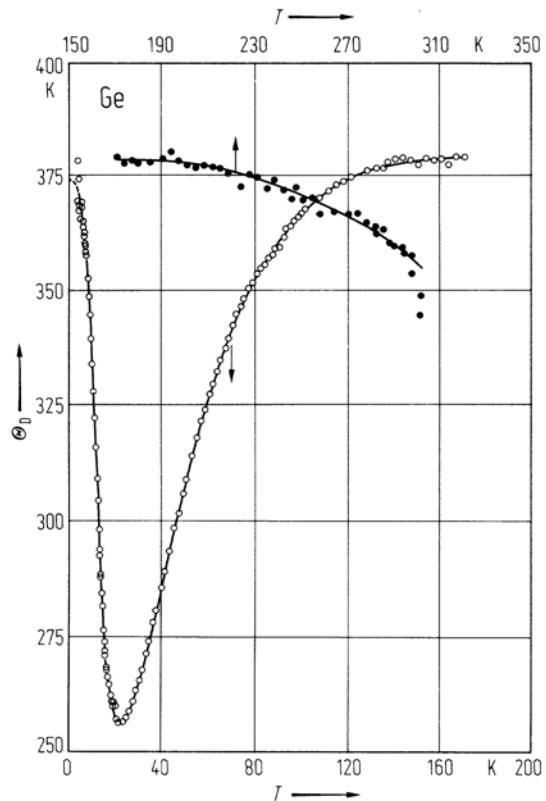


**Fig. 1.3.11**

Ge. Heat capacity at constant volume vs. temperature. Experimental points from [70T], solid line: theoretical [85K].

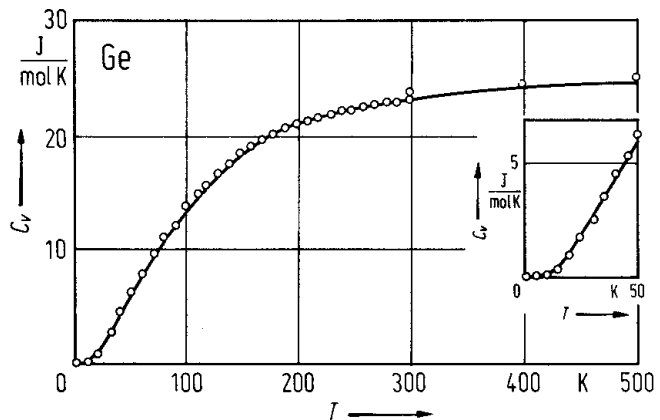


**Fig. 1.3.12**

Ge. Conductivity vs. reciprocal temperature in the range of intrinsic conduction [54M1].

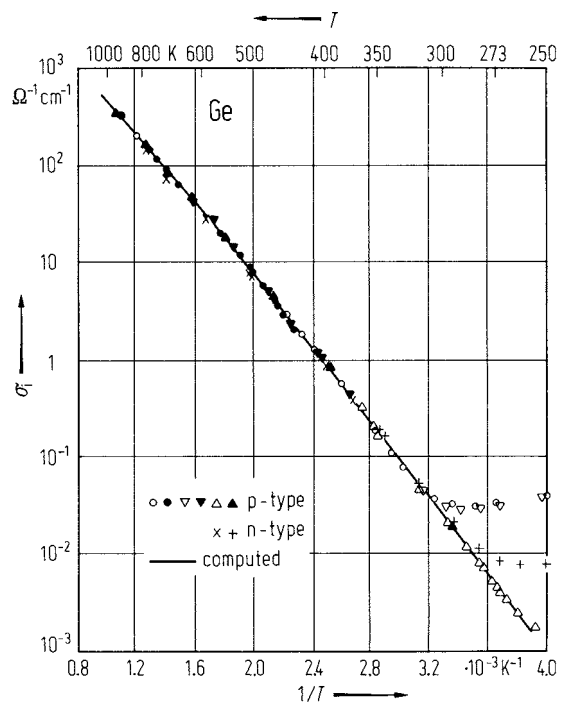


**Fig. 1.3.13**

Ge. Intrinsic carrier concentration vs. reciprocal temperature [54M1].

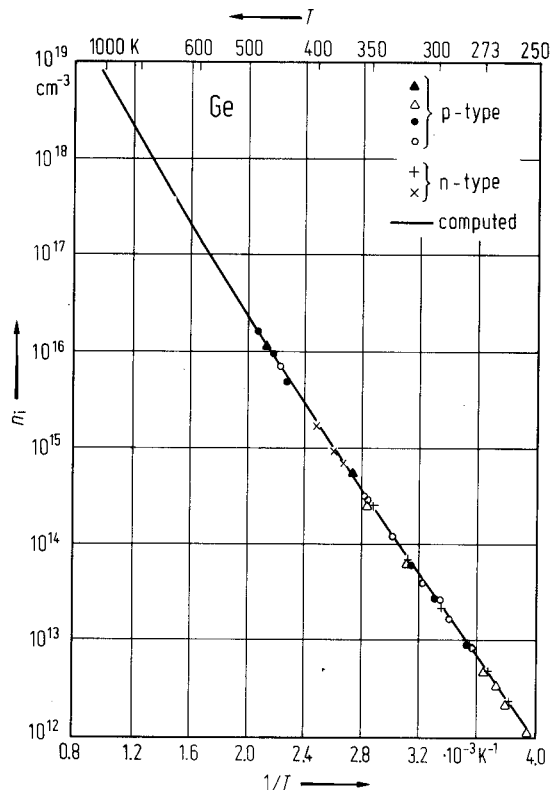


**Fig. 1.3.14**

Ge. (Ohmic) drift mobility of electrons vs. temperature obtained with a time-of-flight technique in hyperpure material (open circles); other symbols: data from five references; solid line: theory [81J].

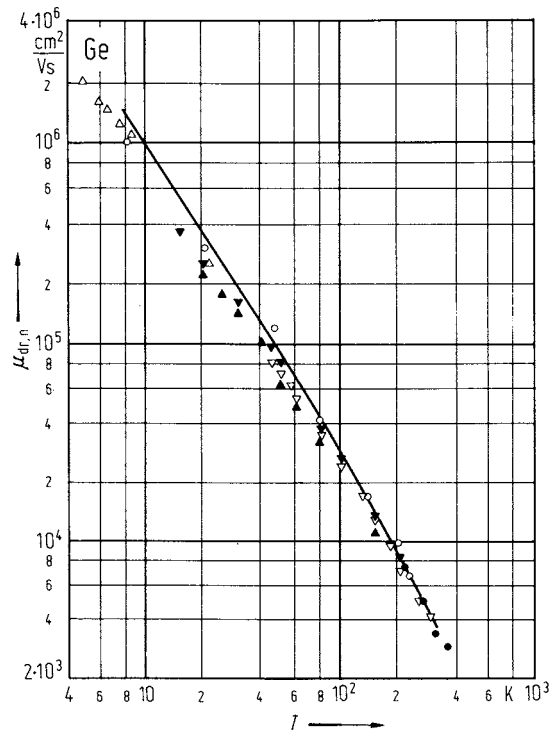


**Fig. 1.3.15**

Ge. Electron and hole mobilities vs. temperature for constant carrier concentration (high purity samples) [54M2].

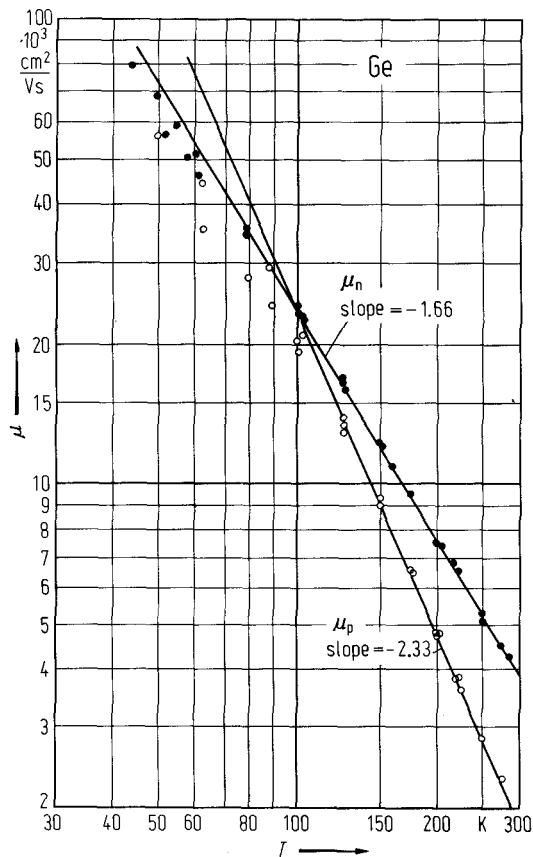


**Fig. 1.3.16**

Ge. Thermoelectric power times temperature vs. temperature. Full triangles:  $n_a = 1.6 \cdot 10^{14} \text{ cm}^{-3}$ ; open circles:  $n_a = 8.0 \cdot 10^{13} \text{ cm}^{-3}$ ; open triangles:  $n_d = 8 \cdot 10^{12} \text{ cm}^{-3}$ ; full circles:  $n_d = 8.9 \cdot 10^{13} \text{ cm}^{-3}$  [54G].

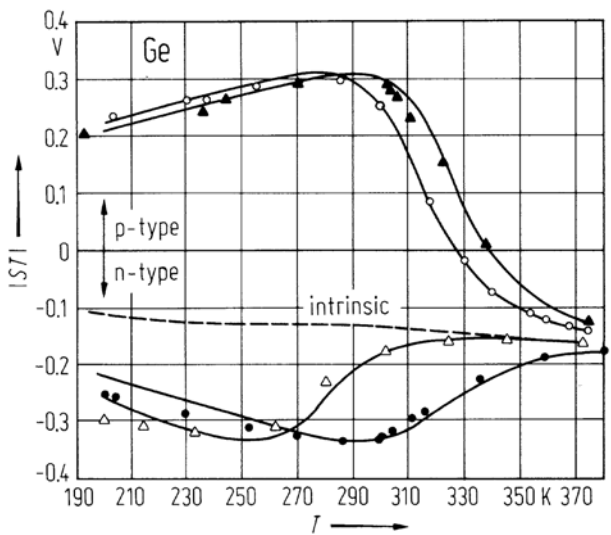


**Fig. 1.3.17**

Ge. Thermal conductivity vs. temperature. (a) 3...400 K, (b) 400...1200 K. Solid curve in (a) and data in (b) from [64G], experimental data in (a) from [84B]. Dashed line in (b): extrapolated lattice component.

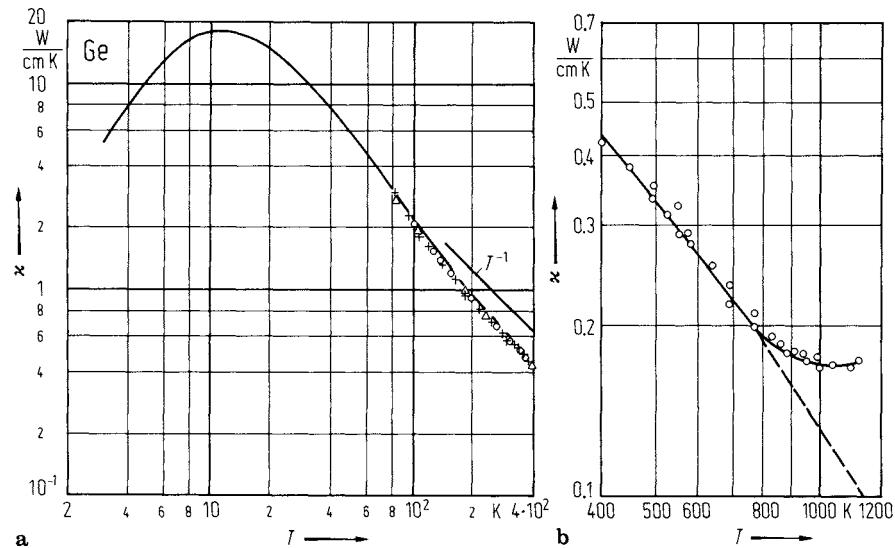


**Fig. 1.3.18**

Ge. Real and imaginary parts of the dielectric constant vs. photon energy [83A2].

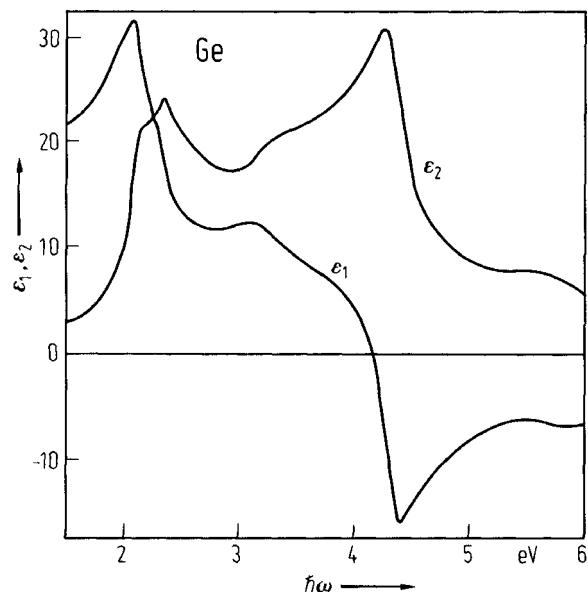


**Fig. 1.3.19**

Ge. Spectral dependence of (a) the refractive index, (b) the extinction coefficient and (c) the absorption coefficient [59P].

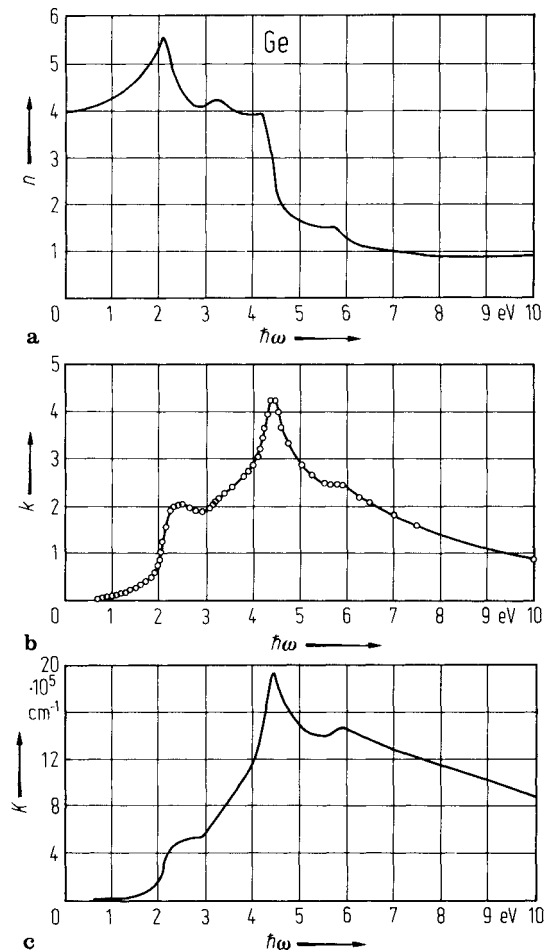


**Fig. 1.3.20**

Ge. Refractive index and extinction coefficient vs. photon energy in the region of the  $E_1$  critical point at 120K [66P].

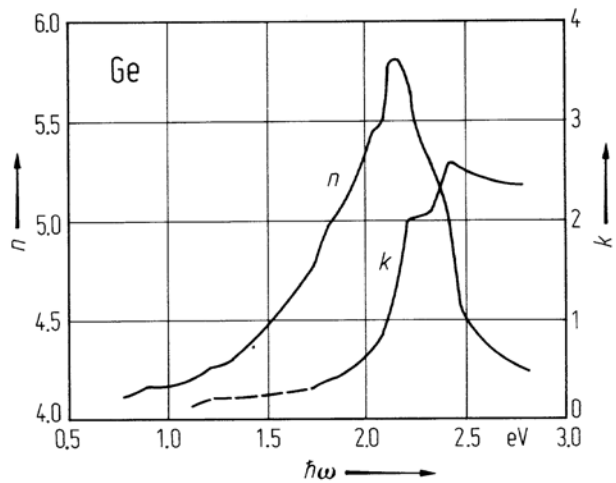


**Fig. 1.3.21**

Ge. Temperature and wavelength dependence of the refractive index. Open circles Curve 1:  $\lambda = 1.970 \mu\text{m}$ ; 2:  $\lambda = 2.190 \mu\text{m}$ ; 3:  $\lambda = 2.409 \mu\text{m}$ ; 4:  $\lambda = 3.826 \mu\text{m}$ ; 5:  $\lambda = 5.156 \mu\text{m}$  [60L].

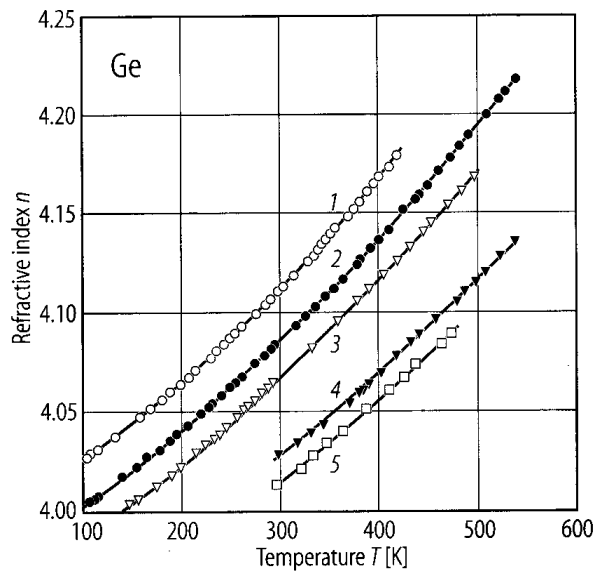


**Fig. 1.3.22**

Ge. Real and imaginary parts of the dielectric constant and energy loss function vs. photon energy [63P].

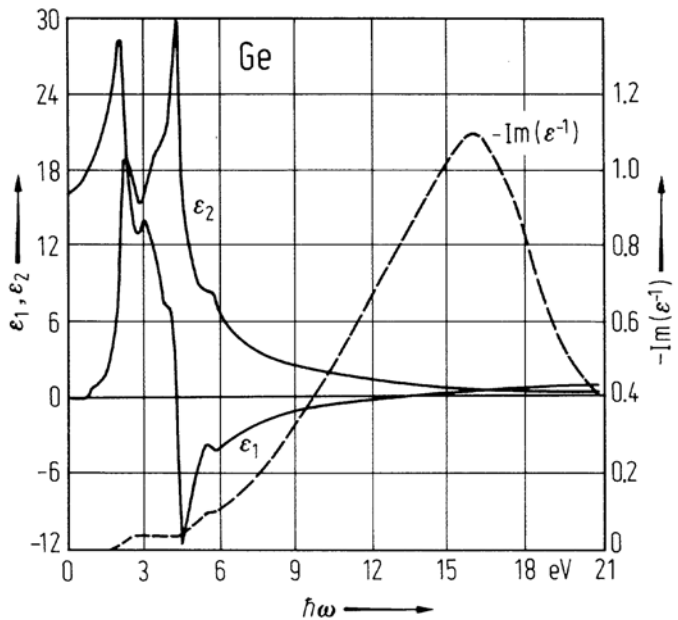


**Fig. 1.3.23**

Ge. Temperature dependence of the high-frequency dielectric constant [96K]. Experimental data points [76I] and ab-initio calculations (full line); dotted line is the theoretical result without the effect of thermal expansion, and dashed line is the full line shifted to match the experimental data.

